Characterization of unipolar electrogram morphology

A novel tool for quantifying conduction inhomogeneity

Ye, Ziliang; Van Schie, Mathijs S.; Pool, Lisa; Heida, Annejet; Knops, Paul; Taverne, Yannick J.H.J.; Brundel, Bianca J.J.M.; De Groot, Natasja M.S.

DOI
10.1093/europace/euad324

Publication date
2023

Document Version
Final published version

Published in
Europace

Citation (APA)
Ye, Z., Van Schie, M. S., Pool, L., Heida, A., Knops, P., Taverne, Y. J. H. J., Brundel, B. J. J. M., & De Groot, N. M. S. (2023). Characterization of unipolar electrogram morphology: A novel tool for quantifying conduction inhomogeneity. *Europace*, *25*(11), Article euad324. https://doi.org/10.1093/europace/euad324

ESC European Society of Cardiology

Europace (2023) **25**, 1–12
https://doi.org/10.1093/europace/euad324

TRANSLATIONAL RESEARCH

Characterization of unipolar electrogram morphology: a novel tool for quantifying conduction inhomogeneity

Ziliang Ye[1], Mathijs S. van Schie [1], Lisa Pool [1], Annejet Heida[1], Paul Knops[1], Yannick J.H.J. Taverne[2], Bianca J.J.M. Brundel[3], and Natasja M.S. de Groot [1,4]*

[1]Department of Cardiology, Erasmus Medical Center, Dr Molewaterplein 40, Rotterdam 3015GD, The Netherlands; [2]Department of Cardiothoracic Surgery, Erasmus Medical Center, Rotterdam, The Netherlands; [3]Department of Physiology, Amsterdam UMC location VU, Amsterdam, The Netherlands; and [4]Department of Microelectronics, Delft University of Technology, Mekelweg 5, 2628CD Delft, The Netherlands

Received 19 September 2023; accepted after revision 21 October 2023; online publish-ahead-of-print 1 November 2023

Aims Areas of conduction inhomogeneity (CI) during sinus rhythm may facilitate the initiation and perpetuation of atrial fibrillation (AF). Currently, no tool is available to quantify the severity of CI. Our aim is to develop and validate a novel tool using unipolar electrograms (EGMs) only to quantify the severity of CI in the atria.

Methods and results Epicardial mapping of the right atrium (RA) and left atrium, including Bachmann's bundle, was performed in 235 patients undergoing coronary artery bypass grafting surgery. Conduction inhomogeneity was defined as the amount of conduction block. Electrograms were classified as single, short, long double (LDP), and fractionated potentials (FPs), and the fractionation duration of non-single potentials was measured. The proportion of low-voltage areas (LVAs, <1 mV) was calculated. Increased CI was associated with decreased potential voltages and increased LVAs, LDPs, and FPs. The Electrical Fingerprint Score consisting of RA EGM features, including LVAs and LDPs, was most accurate in predicting CI severity. The RA Electrical Fingerprint Score demonstrated the highest correlation with the amount of CI in both atria ($r = 0.70$, $P < 0.001$).

Conclusion The Electrical Fingerprint Score is a novel tool to quantify the severity of CI using only unipolar EGM characteristics recorded. This tool can be used to stage the degree of conduction abnormalities without constructing spatial activation patterns, potentially enabling early identification of patients at high risk of post-operative AF or selection of the appropriate ablation approach in addition to pulmonary vein isolation at the electrophysiology laboratory.

* Corresponding author. Tel: +31 10 7035018; fax: +31 10 7035258. *E-mail address*: n.m.s.degroot@erasmusmc.nl

Graphical Abstract

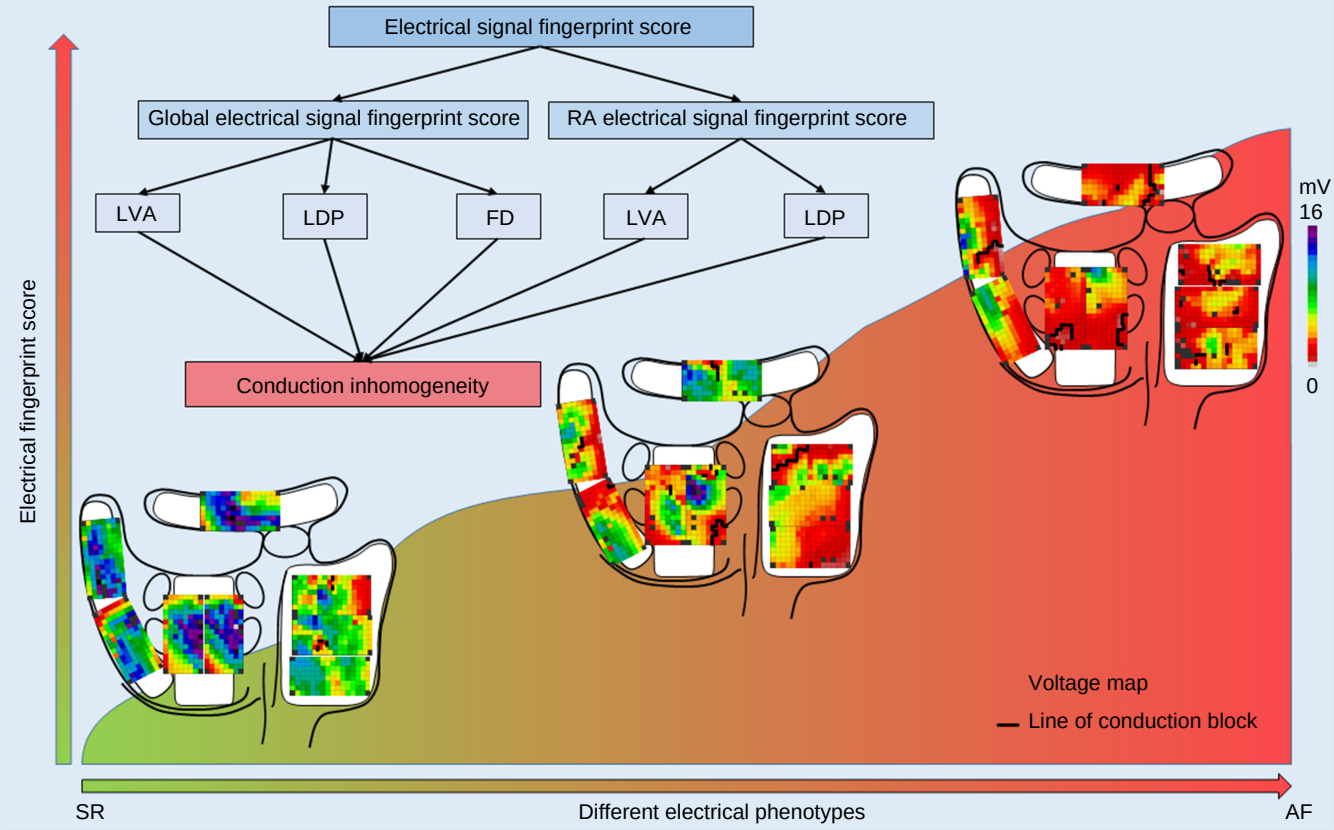

Keywords Conduction inhomogeneity • Atrial fibrillation • Epicardial mapping • Sinus rhythm • Diagnostic tool

What's new?

- An increase in conduction inhomogeneity (CI) is associated with a decrease in potential voltages and increase in low-voltage areas (LVAs), long double potentials (LDPs), and fractionated potentials.
- The Electrical Fingerprint Score consisting of right atrium electrogram (EGM) features, including the amount of LVAs and LDPs, was most accurate in predicting CI severity compared with other atrial regions.
- The individualized Electrical Signal Fingerprint Score as proposed in this study can be used as a novel tool for determining the severity of CI during sinus rhythm using EGMs only, without constructing the spatial patterns of activation.
- Future less- or even non-invasive Electrical Signal Fingerprint Scores may help in early identification of patients at risk of post-operative atrial fibrillation or may aid in the selection of the appropriate ablation approach in addition to pulmonary vein isolation at the electrophysiology laboratory.

Introduction

Conduction disorders, such as slowing of conduction and conduction block (CB), play a role in both the initiation and perpetuation of cardiac arrhythmias.[1] Conduction inhomogeneity (CI) during sinus rhythm (SR) is more pronounced in patients with atrial fibrillation (AF) episodes compared with patients without atrial tachyarrhythmias.[2,3] Prior experimental and clinical studies demonstrated that CI affects electrogram (EGM) morphology and causes low-amplitude, fractionated potentials (FPs).[4–7] Recently, it has been suggested that the so-called Electrical Signal Fingerprint may serve as a potential diagnostic tool to determine the severity and extensiveness of CI.[8] This signal fingerprint contains a large number of quantified unipolar EGM features recorded during SR, such as peak-to-peak amplitudes, fractionation, and EGM duration. However, it is still unknown which EGM features are predictive of CI or whether the EGM features of one atrial region are predictive of other atrial regions. Therefore, the purpose of this study was to further develop the Electrical Signal Fingerprint as a novel, patient-tailored tool to quantify the severity of CI without constructing the spatial patterns of activation, involving various unipolar EGM characteristics.

Methods

Study population

The study population included 235 consecutive adult patients who underwent elective coronary artery bypass grafting (CABG) at the Erasmus Medical Center in Rotterdam, The Netherlands. This study was approved by the Institutional Medical Ethics Committee (MEC2010-054/MEC2014-393).[9,10] Written informed consent was obtained from all patients before enrolment, and patient characteristics (such as age, gender, body mass index, echocardiogram features, medical histories, and comorbidities) were extracted from the patients' medical record system.

Mapping procedure

As previously described, epicardial high-resolution mapping was conducted before the start of extracorporeal circulation.[9,10] A temporal bipolar

epicardial pacemaker wire connected to the right atrial (RA) free wall was used as a reference electrode, and the indifferent electrode made of a steel wire was fixated to the subcutaneous tissue of the thorax.

Epicardial mapping was performed using a 128- or 192-electrode array (electrode diameter 0.65 or 0.45 mm, respectively; and inter-electrode distances 2 mm). During the mapping procedure, the electrode array was shifted across predefined areas at the RA, Bachmann's bundle (BB), and posterior wall of the left atrium (LA) between the pulmonary veins area (PVA) and the LA appendage, as shown in the middle panel of *Figure 1*. The RA was mapped from the cavo-tricuspid isthmus, shifting perpendicular to the caval veins towards the RA appendage. The PVA was mapped from the transverse sinus fold along the margins of the left and right pulmonary veins towards the atrioventricular groove, and the left atrioventricular groove region from the lower margin of the left inferior pulmonary vein towards the LA appendage. Bachmann's bundle was mapped from the roof of the LA appendage across the roof of the LA, behind the aorta towards the superior cavo-atrial junction.

If AF was present at the start of the mapping procedure, electrical cardioversion was conducted to restore SR. A 5 s SR episode was recorded from each mapping site, including a surface electrocardiogram lead, bipolar reference EGM, and all unipolar epicardial EGMs. Recordings were amplified (gain 1000), filtered (bandwidth 0.5–400 Hz), sampled (1 kHz), and analogue-to-digital-converted (16 bits) and then stored on a hard disk.

Data analysis

Customized software was used for performing a semi-automatic analysis of unipolar EGMs. The steepest part of a negative deflection was automatically annotated to construct colour-coded local activation time maps.[11] Recordings were excluded when <30% of the mapping area was annotated. All annotations were manually verified by two investigators. Potential voltage was measured as the peak-to-peak amplitude of the steepest negative deflection. Low-voltage potentials were defined as potentials with an amplitude <1.0 mV.[12] Conduction block was defined as a difference in local activation time between two adjacent electrodes ≥12 ms.[1] The total proportion of CB measured from the entire atrium was used as an indication for the degree of CI.

Consistent with prior mapping studies,[8] EGMs were categorized into single potential (SP), short double potential (SDP), long double potential (LDP), and FP. Fractionation duration (FD) was defined as the time difference between the first and the last deflection of non-SP. As described previously,[13] for SPs, the ratio between the *R*- and the *S*-wave amplitude (*R*/*S* ratio) was calculated, with a scale ranging from −1 (*R*-wave) to 1 (*S*-wave), estimated by the following formula:

$$R/S\ \text{ratio} = \begin{cases} 1 - R/S & \text{for } R/S \le 1 \\ \dfrac{1}{R/S} - 1 & \text{for } R/S > 1 \end{cases}$$

Detection of post-operative atrial fibrillation

Cardiac rhythms of all patients were continuously recorded from the moment of arrival on the surgical ward to the end of the fifth post-operative day using bedside monitors (Draeger Infinity™). Automatic algorithms were used to detect early post-operative AF (E-PoAF) episodes lasting >30 s. All episodes detected by the software were cross-checked by two blinded operators in order to eliminate potential false-positive registrations induced by artefacts.

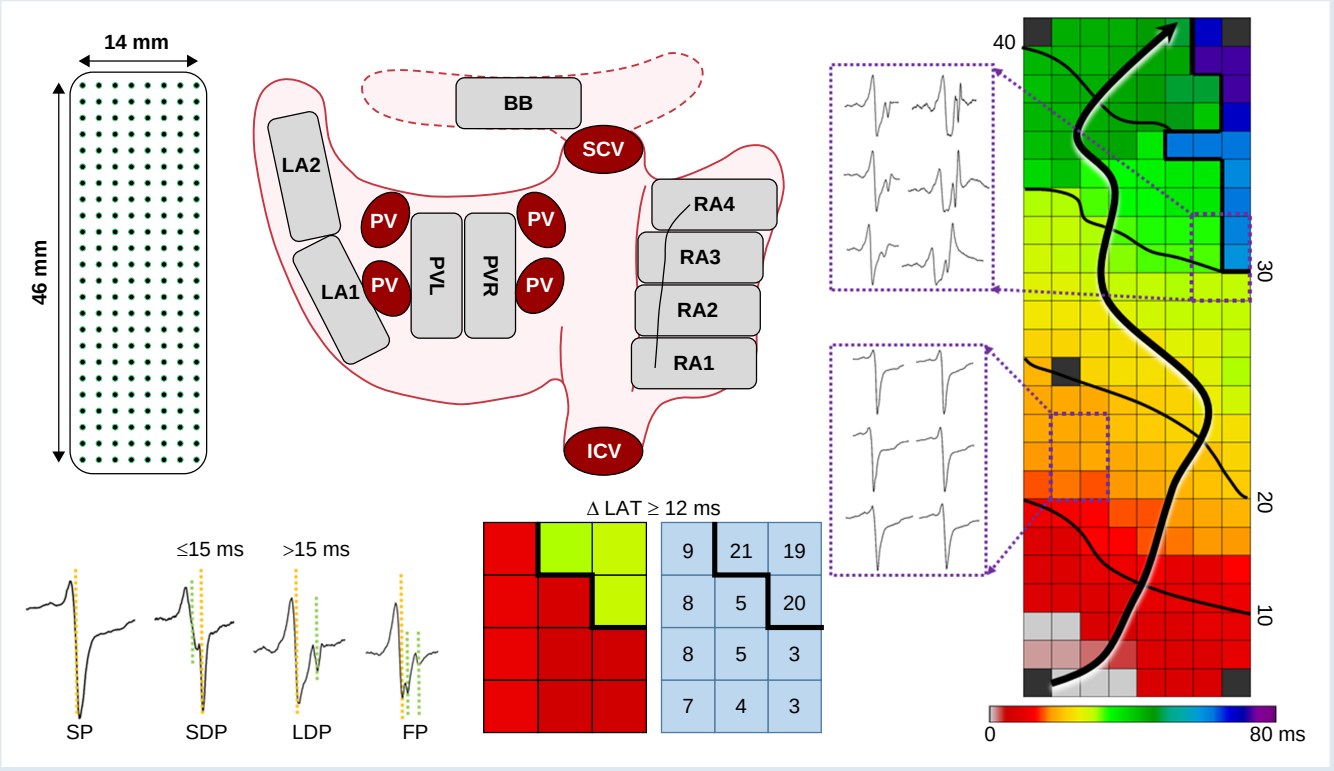

Figure 1 Left upper panel: a 192-unipolar electrode array (left panel) is used for atrial mapping; middle top panel: projection of the electrode array on a schematic posterior view of the entire atria; right panel: a colour-coded activation time map demonstrating both areas of uniform fast conduction and CB. From both areas, unipolar potentials are shown outside the activation time map. Left bottom panel: examples of different potentials. Middle bottom panel: example of a line of CB. Differences in local activation time between two adjacent electrodes ≥12 ms were defined as CB. Isochronal lines (thin black lines) are drawn at 10 ms intervals, and the black arrow indicates the direction of wavefront propagation. BB, Bachmann's bundle; FP, fractionated potential; ICV, inferior caval vein; LA, left atrium; LAT, local activation time; LDP, long double potential; PV, pulmonary vein; PVL, pulmonary vein left; PVR, pulmonary vein right; RA, right atrium; SDP, short double potential; SP, single potential; SCV, superior caval vein.

After the hospitalization period, patients were periodically seen at the outpatient clinic at 3 and 6 months, 1 year, and yearly afterwards for a period of 5 years. The presence of late post-operative AF (L-PoAF) was confirmed by using a surface electrocardiogram or Holter.

Statistical analysis

A Shapiro–Wilk test was used to verify the normal distribution of continuous variables. Continuous variables that were normally distributed are expressed as mean ± standard deviation (SD), while non-normal distributed continuous variables are expressed as median and interquartile range (IQR). Continuous variables among groups were compared using either an independent sample *t*-test or a one-way analysis of variance in case of normal distributed variables and the Mann–Whitney *U* test or Kruskal–Wallis test in the case of non-normally distributed variables.

Categorical variables were described as number and percentage, and a χ^2 test was used for comparison. Pearson or Spearman correlation analysis was used to explore the correlation between variables where appropriate. In addition, univariable and multivariable logistic regression analyses were performed to investigate the variables associated with a higher degree of CI, and the results were presented as odds ratio (OR) with 95% confidence interval. Least absolute shrinkage and selection operator (LASSO) regression analysis was also conducted to further select EGM features associated with a higher degree of CI. Receiver operating characteristic (ROC) curves were constructed to investigate the diagnostic value of EGM features with a high degree of CI. The Electrical Fingerprint Score was constructed using a nomogram approach, using the 'rms' and 'nomogramFormula' packages in R software. This score was calculated based on variables identified as significant in a multivariable logistic regression analysis. A concordance index (*C*-index) was calculated to examine the predictive value of the Electrical Fingerprint Score.

All statistical analyses were completed using IBM SPSS Statistics 28, RStudio (version 4.2.1) and Python (version 3.7). A two-sided *P*-value was considered statistically significant if its value was <0.05.

Results

Study population

As demonstrated in *Figure 2*, the proportion of CB in the entire study population ranged from 0.11 to 7.41% (median: 2.00%). The largest proportion of CB was found at the RA [2.38 (1.18–3.86) %], followed by BB [2.28 (0.86–4.76) %], PVA [1.12 (0.31–2.41) %], and LA [0.76 (0.13–4.76) %]. Based on the 33rd and 66th percentiles of the total proportion of CB, the study population was categorized into three different groups with a low (CB: <1.6%), intermediate (CB: 1.6–2.5%), and high degree of CI (CB: ≥2.5%). The baseline characteristics of the three different patient groups are displayed in *Table 1*. There were no significant differences in baseline characteristics among the three groups, except for age ($P = 0.002$) and diabetes mellitus ($P = 0.011$).

Mapping database

A total of 17 189 heartbeats were recorded, including 2 188 835 potentials (9314 ± 2893 per patient). The average SR cycle length was 885 ± 166 ms. The total number of potentials in the low, intermediate, and high CI groups was, respectively, 696 351, 759 570, and 732 914. Average cycle length did not differ among the three groups (*Table 1*, $P = 0.122$).

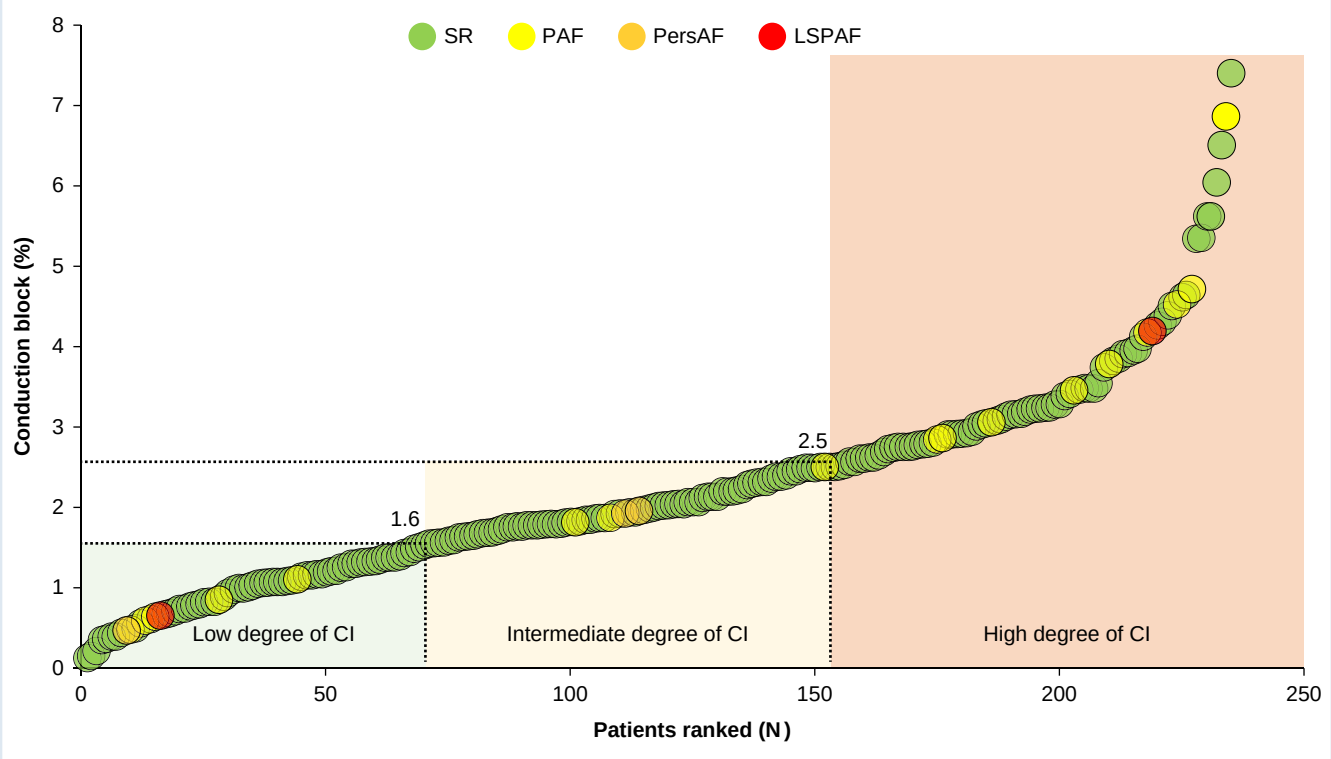

Figure 2 Graph depicting the percentage of CB for each patient individually. The green dots represent patients with SR, whereas the yellow, orange, and red dots represent patients with paroxysmal, persistent, and longstanding persistent AF, respectively. The numbers of 1.6 and 2.5 on the ranking plot correspond to 33 and 66% of CB, respectively. CI, conduction inhomogeneity; LSPAF, long stand persistent atrial fibrillation; PAF, paroxysmal atrial fibrillation; PersAF, persistent atrial fibrillation; SR, sinus rhythm.

Table 1 Baseline characteristics

Variables	Overall	Low CI group	Intermediate CI group	High CI group	*P*-value
n	235	78	77	80	
Range of CB, %		CB < 1.6	1.6 ≤ CB < 2.5	CB ≥ 2.5	
Age (median and IQR, years)	67 (60, 73)	64 (57, 69)	69 (64, 75)	68 (60, 74)	0.002
Male, *n* (%)	198 (84.3)	70 (89.7)	65 (84.4)	63 (78.8)	0.165
BMI (median and IQR, kg/m^2)	27.6 (25.5, 31.1)	27.4 (25.1, 31.2)	27.7 (25.7, 30.8)	27.9 (25.8, 31.3)	0.719
Type of AF, *n* (%)					0.396
No AF	213 (90.6)	71 (91.0)	72 (93.5)	70 (87.5)	
Paroxysmal AF	17 (7.2)	5 (6.4)	3 (3.9)	9 (11.2)	
Persistent AF	3 (1.3)	1 (1.3)	2 (2.6)	0 (0.0)	
Longstanding persistent AF	2 (0.9)	1 (1.3)	0 (0.0)	1 (1.2)	
Hypertension, *n* (%)	148 (63.0)	43 (55.1)	54 (70.1)	51 (63.7)	0.152
Dyslipidaemia, *n* (%)	103 (43.8)	28 (35.9)	32 (41.6)	43 (53.8)	0.069
Diabetes mellitus, *n* (%)	81 (34.5)	17 (21.8)	29 (37.7)	35 (43.8)	0.011
Myocardial infarction, *n* (%)	116 (49.4)	44 (56.4)	38 (49.4)	34 (42.5)	0.217
Left ventricular function, *n* (%)					0.739
Normal (EF >55%)	174 (74.0)	56 (71.8)	59 (76.6)	59 (73.8)	
Mild impairment (EF 46–55%)	50 (21.3)	18 (23.1)	13 (16.9)	19 (23.8)	
Moderate impairment (EF 36–45%)	8 (3.4)	3 (3.8)	3 (3.9)	2 (2.5)	
Severe impairment (EF <35%)	3 (1.3)	1 (1.3)	2 (2.6)	0 (0.0)	
Left atrial dilatation > 45 mm, *n* (%)	32 (13.6)	8 (10.3)	8 (10.4)	16 (20.0)	0.304
ACEI/ARB/AT2 antagonist, *n* (%)	159 (67.9)	61 (78.2)	47 (61.8)	51 (63.7)	0.057
Statin, *n* (%)	207 (88.1)	69 (88.5)	69 (89.6)	69 (86.2)	0.803
Digoxin, *n* (%)	3 (1.3)	0 (0.0)	1 (1.3)	2 (2.5)	0.376
Class I, *n* (%)	0 (0.0)	0 (0.0)	0 (0.0)	0 (0.0)	NA
Class II, *n* (%)	183 (77.9)	60 (76.9)	60 (77.9)	63 (78.8)	0.962
Class III, *n* (%)	9 (3.8)	4 (5.1)	2 (2.6)	3 (3.8)	0.713
Class IV, *n* (%)	11 (4.7)	3 (3.8)	4 (5.2)	4 (5.0)	0.911
Cycle length (mean ± SD, ms)	885 ± 166	870 ± 165	864 ± 161	918 ± 166	0.122

ACEI, angiotensin-converting enzyme inhibitors; AF, atrial fibrillation; ARB, angiotensin receptor blockers; AT2, angiotensin Type 2 receptor; BMI, body mass index; CB, conduction block; CI, conduction inhomogeneity; EF, ejection fraction; IQR, interquartile range; NA, not available; SD, standard deviation.

Conduction inhomogeneity and median potential voltages

Figure 3 illustrates representative examples of unipolar potential voltage maps obtained from two patients from each of the three groups. These voltage maps show lower unipolar potential voltages and more low-voltage areas (LVAs) in patients with a higher degree of CI, although there was no predilection site for LVAs to occur.

The left panel of *Figure 4* shows differences in median potential voltages among the three groups for the entire atria and each atrial region separately. For the entire atria, median potential voltages were lower in the high CI group [low: 5.73 (5.05–6.87) mV; intermediate: 4.70 (3.98–5.69) mV; high: 4.03 (3.49–4.96) mV; $P < 0.05$ for each comparison], while the amount of LVAs was highest in the high CI group [high: 9.49 (6.12–12.99) %, intermediate: 5.67 (3.76–9.32) %, and low: 3.21 (1.81–5.64), $P < 0.05$ for each comparison, right panel of *Figure 4*].

Supplementary material online, *Table S1* summarizes the magnitudes of median potential voltages and proportions of LVAs for each region separately, demonstrating that the highest median potential voltages were observed in the patients of the low CI group and the largest proportion of LVAs in the high CI group; this trend was, however, not found at the LA.

Conduction inhomogeneity and potential morphology

For the entire atria, patients with a high degree CI had the lowest proportion of SPs [high: 78.88 (74.11, 82.57) %; low: 85.77 (81.98, 89.84) %; $P < 0.001$]. A higher degree CI was also associated with a significant increase in the proportion of LDPs [high: 6.24 (4.59, 8.07) %; low: 1.82 (1.13, 3.20) %; $P < 0.001$] and FPs [high: 2.47 (1.47, 3.92) %; low: 1.25 (0.59, 2.02) %; $P < 0.001$]. However, there was no relationship between the degree of CI and the proportion of SDPs ($P > 0.05$).

Figure 5 illustrates the proportion of the different types of potentials in the three groups for each atrial region separately. As expected, the lowest proportions of SPs were found in the high CI group, although there was no difference in the proportion of SPs recorded from the PVA among the three groups (see Supplementary material online, *Table S2*). A high proportion of LDPs in each region was related to a

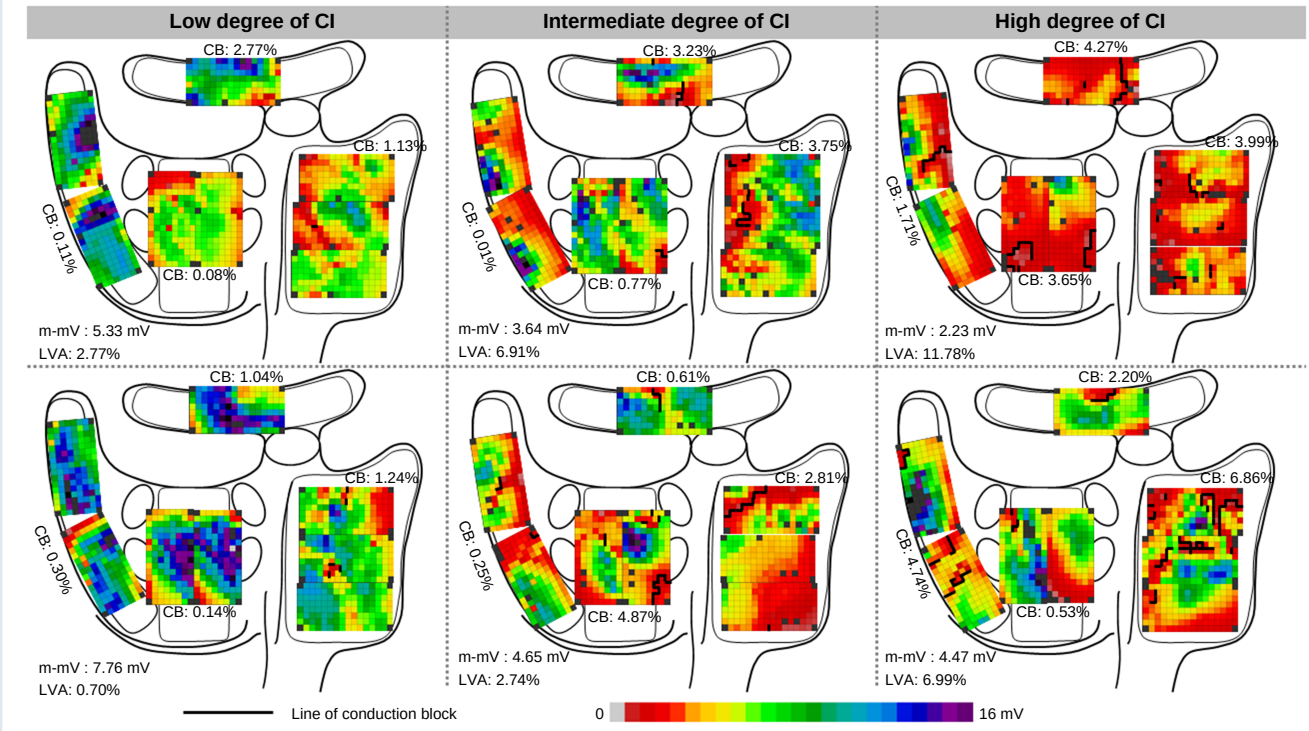

Figure 3 Graph illustrating representative examples of unipolar voltage maps obtained from two patients from each of the three groups. Left panel: maps obtained from two patients of the low CI group, and the total amount of CB was 0.79 and 0.73%, respectively. Middle panel: maps obtained from two patients of the intermediate CI group (the amount of CB was 2.35 and 2.29%, respectively); right panel: maps obtained from two patients of the high CI group (CB was 3.44 and 4.39%, respectively). In general, unipolar voltages decrease when CB increases. CB, conduction block; CI, conduction inhomogeneity; LVA, low-voltage area; m-mV, median unipolar potential voltage.

high degree of CI. An increase in CI was associated with a higher proportion of FPs at the RA, BB, and LA. However, there was no relationship between the degree of CI and the proportion of FPs at the PVA ($P = 0.887$). The amount of SDPs did not differ in any region among the three groups ($P > 0.05$ for each comparison).

Conduction inhomogeneity and *R/S* ratio

Comparisons of *R/S* ratios among the three groups for the entire atria and each region separately are summarized in Supplementary material online, *Table S3*. The *R/S* ratio differed among the three groups only in the RA region ($P = 0.017$).

Conduction inhomogeneity and fractionation duration

Fractionation duration was longer in the high CI group than in the low CI group. This was observed for the entire atria ($P < 0.001$) and also for each region separately (RA: $P < 0.001$; BB: $P < 0.001$; PVA: $P = 0.004$; and LA: $P = 0.004$), as summarized in Supplementary material online, *Table S3*.

Regional interdependency of electrogram features

Table 2 demonstrates the correlations of all EGM features among the various atrial regions; all correlation coefficients are either too weak and/or not significant, indicating that, unfortunately, EGM features assessed in one specific region are not predictive for the features of EGMs recorded in other regions.

Selection of electrogram features for electrical signal fingerprint

In order to construct an Electrical Signal Fingerprint Score for predicting the degree of CI in each individual patient, patients in the low and intermediate CI groups were combined and compared with those in the high CI group. The results of the univariable logistic regression for the potential determinants of a high degree of CI are displayed in Supplementary material online, *Table S4*. To identify the parameters related to a high degree of CI, EGM features associated with a high degree of CI in univariable regression were further included in a LASSO regression analysis. Based on the LASSO analysis, the following EGM features were identified LVA, SP, LDP, and FD (entire atria, Supplementary material online, *Figure S1*), LVA and LDP (RA, Supplementary material online, *Figure S2*), median potential voltage, LDP, and FP (BB, Supplementary material online, *Figure S3*); median potential voltage and LDP (PVA, Supplementary material online, *Figure S4*); LDP and FP (LA, Supplementary material online, *Figure S5*). These EGM features were entered into multivariable regression models, and their results are listed in *Table 3*. For the entire atria, the amount of LVAs (OR = 1.26, $P < 0.001$), the proportion of LDPs (OR = 1.79, $P = 0.003$), and FD (OR = 1.45, $P = 0.017$) were associated with a higher degree of CI. For RA EGM features, the amount of LVAs (OR = 1.13, $P < 0.001$) and the proportion of LDPs (OR = 1.32, $P < 0.001$) were associated with a higher degree of CI. For BB, PVA, and LA, an increased proportion of LDPs

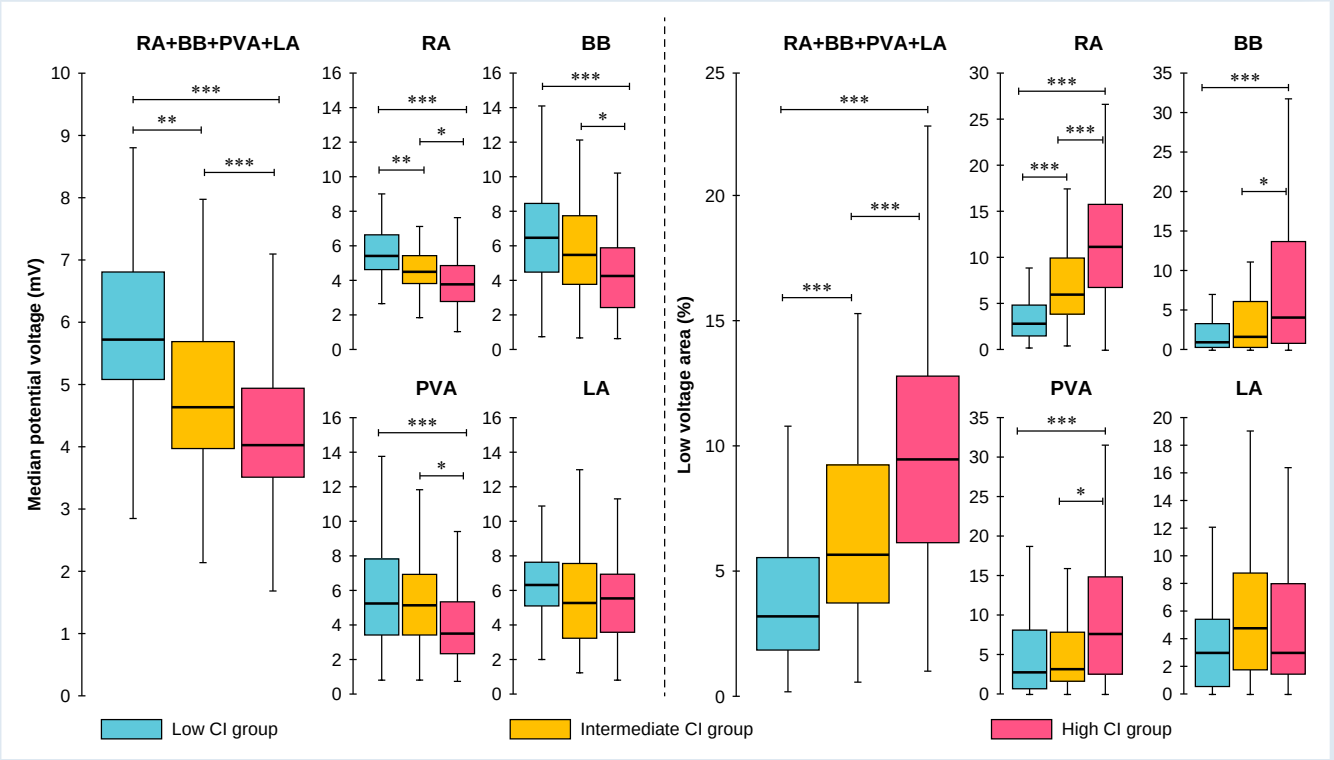

Figure 4 Boxplots comparing the differences in median potential voltage and LVA among the three groups in each atrial region. *$P < 0.05$; **$P < 0.01$; ***$P < 0.001$. BB, Bachmann's bundle; CI, conduction inhomogeneity; LA, left atrium; PVA, pulmonary vein area; RA, right atrium.

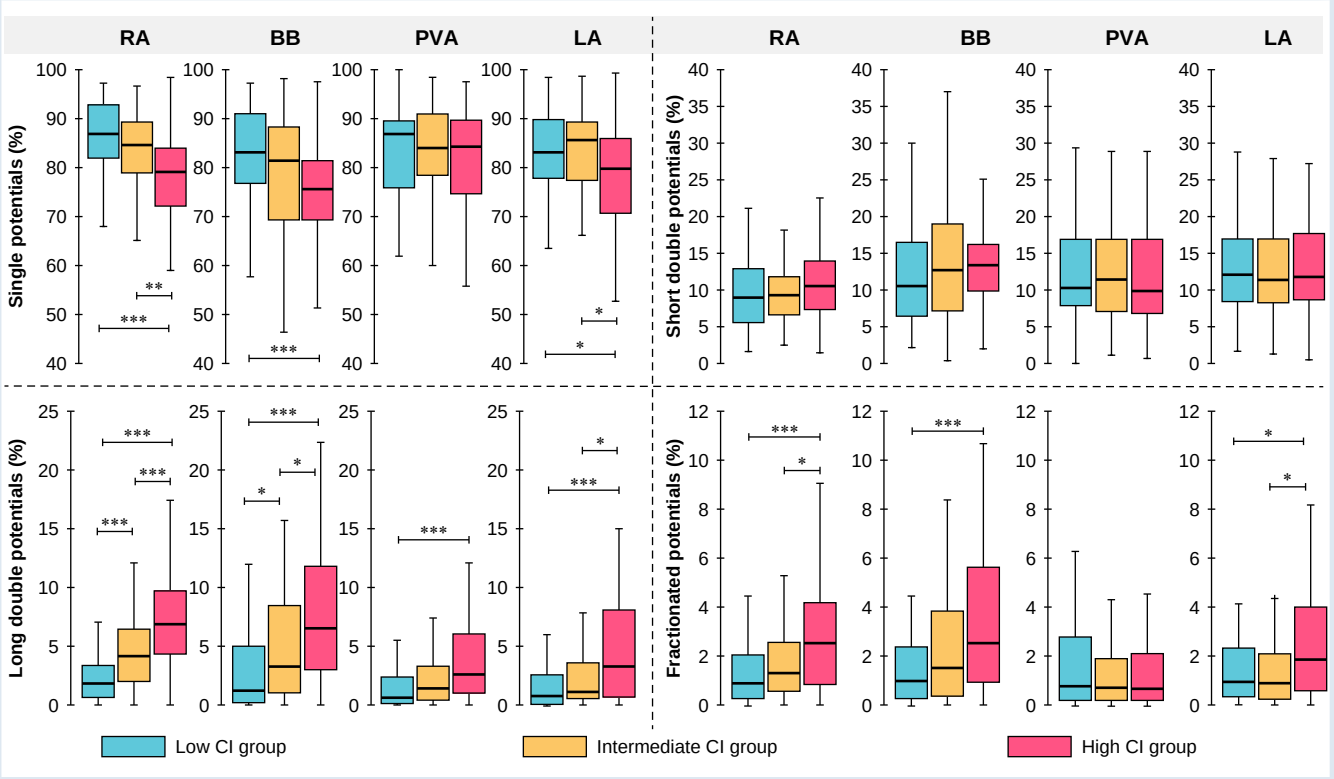

Figure 5 Boxplots evaluating the differences in different atrial morphologies among the three groups in each atrial region. *$P < 0.05$; **$P < 0.01$; ***$P < 0.001$. BB, Bachmann's bundle; CI, conduction inhomogeneity; LA, left atrium; PVA, pulmonary vein area; RA, right atrium.

Table 2 Regional interdependency of electrogram features

	RA	BB	PVA	LA
Median potential voltage				
RA	1	0.344[a]	0.194[a]	0.251[a]
BB	0.344[a]	1	0.121	0.137
PV	0.194[a]	0.121	1	0.235[a]
LA	0.251[a]	0.137	0.235[a]	1
Low-voltage area				
RA	1	0.327[a]	0.216[a]	0.209[a]
BB	0.327[a]	1	0.01	0.156[b]
PV	0.216[a]	0.01	1	0.145[b]
LA	0.209[a]	0.156[b]	0.145[b]	1
RS ratio				
RA	1	0.058	−0.088	−0.143[b]
BB	0.058	1	−0.128	−0.041
PV	−0.088	−0.128	1	0.112
LA	−0.143[b]	−0.041	0.112	1
SP				
RA	1	0.208[a]	0.081	0.172[b]
BB	0.208[a]	1	0.02	0.114
PV	0.081	0.02	1	0.192[a]
LA	0.172[b]	0.114	0.192[a]	1
SDP				
RA	1	0.180[b]	0.102	0.228[a]
BB	0.180[b]	1	0.116	0.038
PV	0.102	0.116	1	0.218[a]
LA	0.228[a]	0.038	0.218[a]	1
LDP				
RA	1	0.177[b]	0.016	−0.034
BB	0.177[b]	1	−0.008	0.153[b]
PV	0.016	−0.008	1	0.059
LA	−0.034	0.153[b]	0.059	1
FP				
RA	1	0.234[a]	0.131	0.179[b]
BB	0.234[a]	1	0.118	0.177[b]
PV	0.131	0.118	1	0.261[a]
LA	0.179[b]	0.177[b]	0.261[a]	1
FD				
RA	1	0.068	0.088	−0.095
BB	0.068	1	0.01	0.169[b]
PV	0.088	0.01	1	0.079
LA	−0.095	0.169[b]	0.079	1

BB, Bachmann's bundle; FD, fractionation duration; FP, fractionated potential; LA, left atrium; LDP, long double potential; PVA, pulmonary vein area; RA, right atrium; SDP, short double potential; SP, single potential.
[a]Correlation is significant at the 0.01 level (two-tailed).
[b]Correlation is significant at the 0.05 level (two-tailed).

(BB: OR = 1.09; PVA: OR = 1.07; LA: OR = 1.10) was associated with a higher degree of CI. In addition, median potential voltage (OR = 0.89, $P = 0.041$) at the PVA and the proportion of FPs (OR = 1.18, $P = 0.025$) at the LA were associated with a higher degree of CI.

Table 3 Electrogram features independently associated with a high degree of conduction inhomogeneity

Variables	OR	95% CI	*P*-value
Entire atrium			
LVA	1.26	1.13–1.41	<0.001
LDP	1.79	1.23–2.66	0.003
FD	1.45	1.08–2.00	0.017
RA			
LVA	1.13	1.07–1.20	<0.001
LDP	1.32	1.20–1.48	<0.001
BB			
LDP	1.09	1.03–1.16	0.005
PVA			
Median potential voltage	0.89	0.79–0.99	0.041
LDP	1.07	1.01–1.15	0.023
LA			
LDP	1.10	1.03–1.20	0.012
FP	1.18	1.02–1.37	0.025

BB, Bachmann's bundle; CI, confidence interval; FD, fractionation duration; FP, fractionated potential; LA, left atrium; LDP, long double potential; LVA, low-voltage area; OR, odds ratio; PVA, pulmonary vein area; RA, right atrium.

As demonstrated by the ROC curves for the entire atria in *Figure 6*, the combination of LDP, FD, and LVA has an excellent predictive value for a high degree of CI [area under the curve (AUC) = 0.92]. In addition, EGM features recorded at the RA have a high predictive value for a high degree of CI (AUC = 0.83), while EGM features recorded in the other regions do not have adequate predictive values.

The electrical signal fingerprint score

Figure 7 demonstrates the Global Electrical Signal Fingerprint Score based on the EGM features obtained from the entire atria [*C*-index: 0.92 (0.89, 0.95)]. The Regional Electrical Signal Fingerprint Scores for the prediction of the total degree of CI in the entire atria are shown in Supplementary material online, *Figure S6*. As demonstrated in this figure, EGM features obtained from the RA had the highest predictive value for the total amount of CI [*C*-index: 0.83 (0.78, 0.89)], followed by BB [*C*-index: 0.69 (0.61, 0.76)], PVA [*C*-index: 0.68 (0.60, 0.75)], and LA [*C*-index: 0.68 (0.60, 0.76)].

Individual signal electrical fingerprint score

The next step was to validate the Electrical Signal Fingerprint Scores by calculating the scores for each patient individually. As illustrated in *Figure 8*, the Global Electrical Signal Fingerprint Score was strongly related to the total degree of CI ($r = 0.82$, $P < 0.001$). Using the Regional Electrical Signal Fingerprint Scores, only EGM features recorded at the RA were strongly related to the total degree of CI ($r = 0.70$, $P < 0.001$). Moderate or weak correlations were found between the total degree of CI and Electrical Signal Fingerprint Scores computed from BB, PVA, and LA ($r = 0.42$, $r = 0.30$, and $r = 0.31$, respectively; $P < 0.001$ for each).

Relationship with post-operative atrial fibrillation

Data on post-operative AF (PoAF) were available in 203 patients of whom 89 developed E-PoAF (43.8%) and 10 L-PoAF (4.9%). The

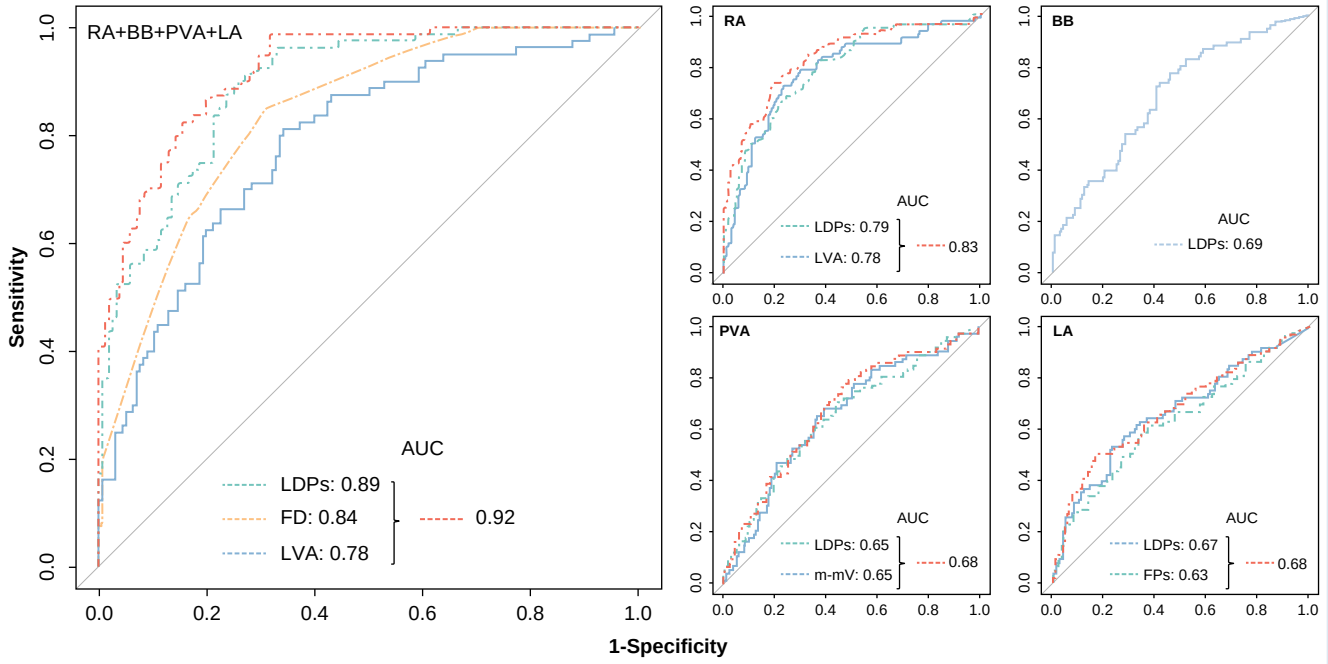

Figure 6 ROC curves calculated by using the EGM features recorded from the whole atrium and regional atrium in the diagnosis of a high degree of CI. AUC, area under the curve; BB, Bachmann's bundle; FD, fractionation duration; FPs, fractionated potentials; LA, left atrium; LDPs, long double potentials; LVA, low-voltage area; m-mV, median unipolar potential voltage; PVA, pulmonary vein area; RA, right atrium.

Global Electrical Signal Fingerprint Score was increased in patients who developed E-PoAF [without PoAF: 42.9 (27.7–64.6) vs. E-PoAF: 50.3 (31.0–63.7), $P < 0.001$] and even more in patients who developed L-PoAF [63.1 (39.3–70.3), $P < 0.001$]. The Regional Electrical Signal Fingerprint Score of the RA was increased only in patients who developed L-PoAF [without PoAF: 22.8 (12.5–43.5) vs. E-PoAF: 25.1 (14.0–43.1), $P = 0.500$ and L-PoAF: 39.8 (23.1–43.3), $P < 0.001$].

Discussion

Key findings

The severity of CI can be accurately predicted by using a Global Electrical Fingerprint Score, containing quantified features of EGM morphology obtained from the entire atria, including the amount of LVA, LDP, and FD. Conduction inhomogeneity in the entire atria can also be predicted with the Regional Electrical Signal Fingerprint Score of the RA, containing the amount of LVAs and LDPs.

Conduction inhomogeneity and potential voltages

Although unipolar potential voltages are affected by numerous factors, Spach *et al.*[7] demonstrated in a dog model that fast conduction is characterized by high-voltage biphasic deflections, while low-voltage, triphasic deflections were recorded during slow conduction.[14,15] In patients with mitral valve disease, it was demonstrated that smaller voltages were indeed recorded in areas of conduction slowing but also around the lines of CB.[12,13] In our previous study, we demonstrated that the presence of LVAs was strongly related to the occurrence of CB at the RA and BB.[8] The presence of extensive areas of CB could therefore result in a decrease in median unipolar potential voltage and increase in LVAs. We now demonstrated that a higher total degree of CI was indeed related to lower unipolar potential voltages and a larger amount of LVAs and was an important parameter integrated in the Electrical Signal Fingerprint Scores.

Conduction inhomogeneity and potential morphology

As described by Konings *et al.*,[16] unipolar potentials are classically categorized into SPs, SDPs, LDPs, and FPs. The morphology of SPs can be further described by the ratio between a positive *R*-wave and a negative *S*-wave, respectively, preceding and following the negative deflection (*R*/*S* ratio).[13] We did not find a correlation between the *R*/*S* ratio and CI. Prior mapping studies demonstrated that during SR, the *R*/*S* ratios of unipolar SPs were considerably variable and that high-voltage SPs were mainly recorded during fast, uniform wavefront propagation.[13,16] In patients with AF, there was a loss of *S*-wave amplitude resulting in SPs with lower amplitudes and shifted *R*/*S* ratios, which was also associated with reduced conduction velocity. In case of extensive CI, more LDPs instead of SPs are recorded. The *R*/*S* ratios of the remaining SPs could therefore be changed only minimally, as they are recorded further away from the lines of CB. Indeed, the amount of LDPs was predictive for the total degree of CI.

Although a substantial proportion of SDPs and even LDPs reflect the physiological heterogeneity of atrial tissue, LDPs and particularly FPs have been associated with CI. During AF at the RA, Konings *et al.*[16] demonstrated that LDPs and FPs were predominantly found near areas of CB. It is therefore not surprising that the proportions of LDPs and FPs were correlated to CI. The duration of FPs was also associated with CI. As demonstrated by previous studies, potentials with a prolonged FD are associated with local areas of impaired conduction.[17,18] A prolonged FD also indicates that a wavefront takes longer to propagate around a line of CB and activate the other side. With more and longer lines of CB, the delay of the wavefront is also more likely to increase.

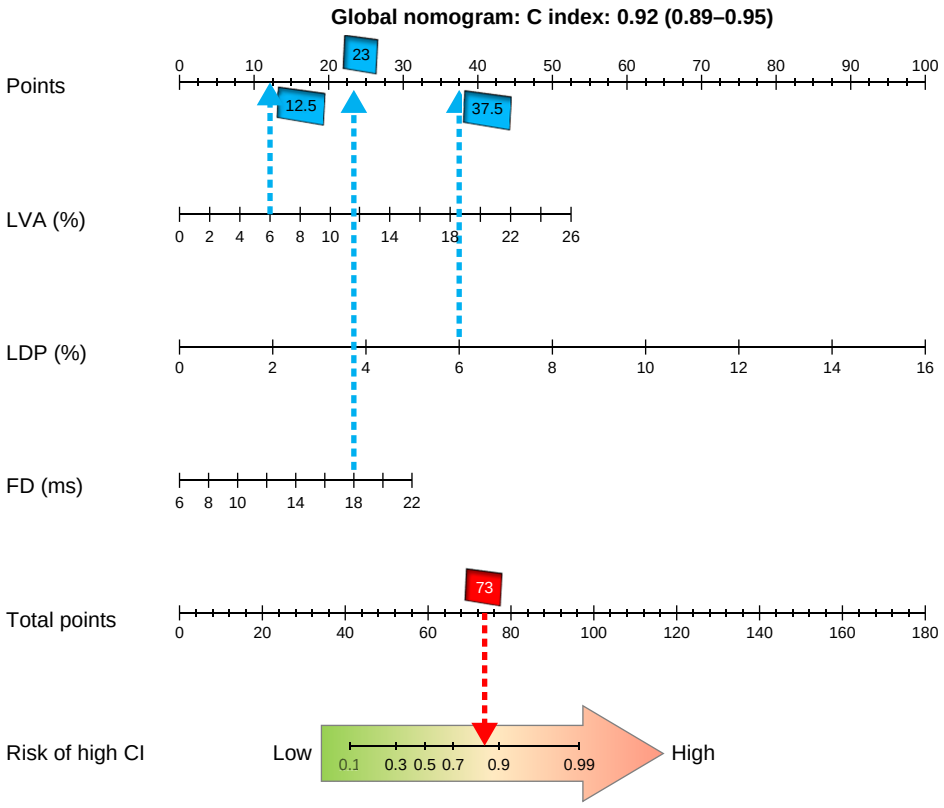

Figure 7 Nomogram for quantifying the severity of CI in the entire atria. The influence of each parameter on the nomogram predicting the risk of high CI is exhibited on the horizontal axes of variable lengths. The usage of this nomogram is described below: chose a specific value of one parameter and draw a vertical line up to 'Points' to determine the score of this parameter earned. The sum of those scores corresponding to the 'Total Points' axis on the bottom and another vertical line is drawn up to the axis of 'Risk of high conduction inhomogeneity' to determine the risk of high CI. CI, conduction inhomogeneity; FD, fractionation duration; LDP, long double potential; LVA, low-voltage area.

Our results indeed showed that prolongation of FPs was related to a higher degree of CI.

The role of the right atrium in signal fingerprinting

Remarkably, our study demonstrated that the severity and extensiveness of CI in the *entire* atria can be estimated using EGM features recorded only from the RA. In a previous mapping study of Lanters *et al.*,[19] the superior inter-caval region was found to be a predilection site for CB in patients with coronary artery disease without AF. Heida *et al.*[20] showed that patients with a history of AF have more severe conduction disorders at the RA and BB. In the current study, a certain degree of CB at the RA was present in each patient. When structural remodelling occurs in the (right) atria, the degree of CI increases, thereby increasing the amount of LDPs and FPs and decreasing unipolar potential voltages. It is believed that atrial structural remodelling plays an important role in the initiation and perpetuation of AF, although most studies mainly focus on the LA. In patients undergoing ablation therapy for persistent AF, Prabhu *et al.*[21] demonstrated that AF is associated with remodelling processes affecting both atria and that electrical and structural remodelling within the RA correlated with the LA. Recently, Heida *et al.*[22] were the first to investigate conduction disorders caused by AF-related electrical remodelling immediately after electrical cardioversion and demonstrated that there was no significant impairment in intra-atrial conduction when compared with conduction patterns observed during long periods of SR. Also, Takagi *et al.*[23] recently demonstrated that only structural remodelling in the RA was a useful predictor of clinical outcome after pulmonary vein isolation. It could be that structural remodelling in the RA more easily results in changes in EGM morphology, as the RA is not uniform in thickness due to the trabeculated wall. This might explain why the RA is a good predictor for the general degree of CI across both atria using unipolar EGM morphology characteristics.

Future clinical implications

Areas of CI identified during SR may play a pivotal role in the initiation and maintenance of atrial tachyarrhythmias such as AF.[24,25] Heida *et al.*[20] indeed showed that patients with AF have more severe CI than patients without prior AF episodes. The individualized Electrical Signal Fingerprint Score as proposed in this study can be used as a novel tool for determining the severity of CI during SR using only EGMs, without constructing the spatial patterns of activation. We also demonstrated that an increased Electrical Signal Fingerprint Score is related to the development of PoAF. The next step will be to test whether this SR Electrical Signal Fingerprint Score can actually predict AF development during short- and long-term follow-up or whether it can predict AF recurrences of arrhythmia surgery outcome.

The high-resolution, invasive gold standard Electrical Signal Fingerprint Score is also the foundation for the development of less- or even non-invasive fingerprints. In patients undergoing cardiac

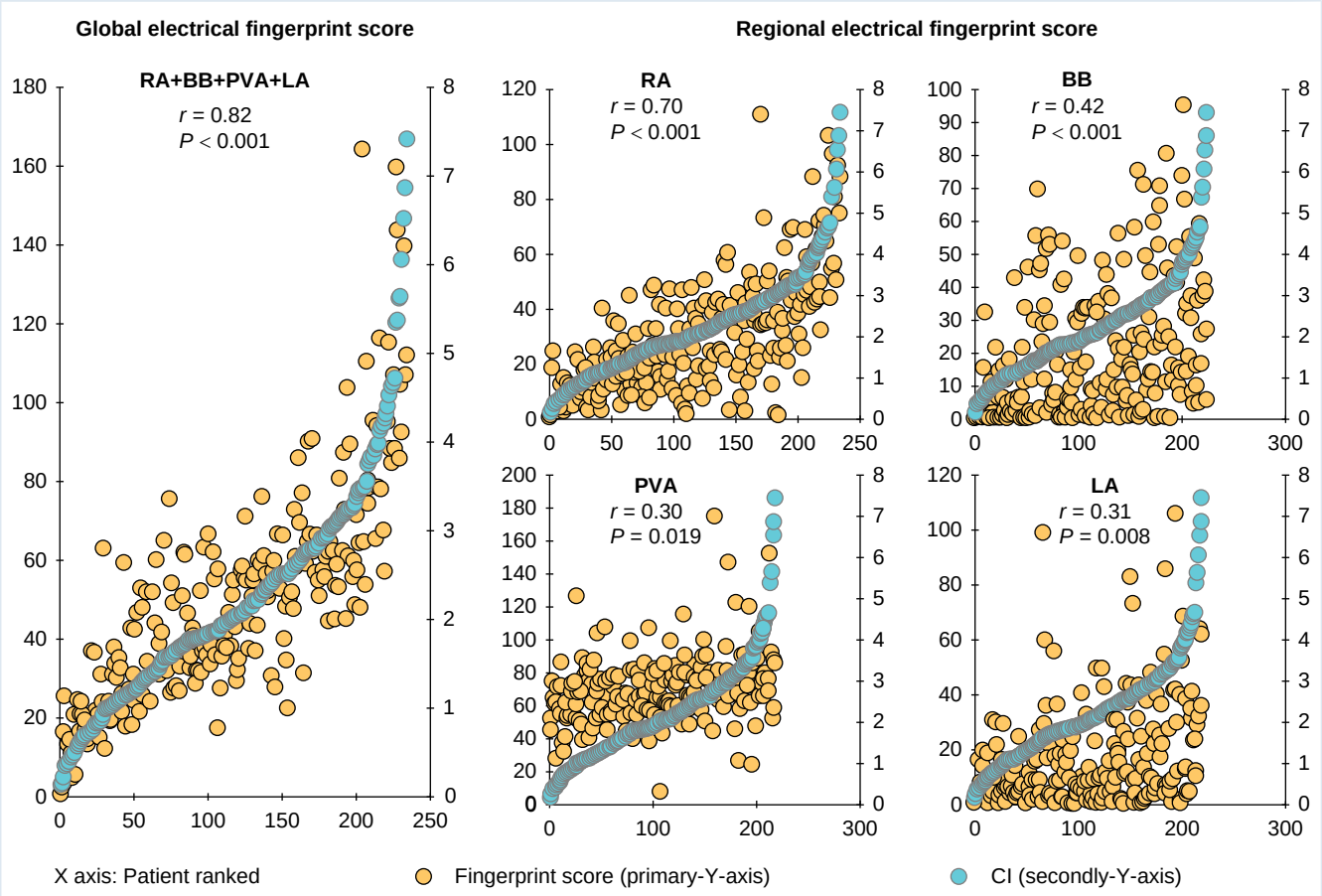

Figure 8 Correlation of the Global Electrical Fingerprint Score and Regional Electrical Signal Fingerprint Score and CB in the individual patient. BB, Bachmann's bundle; CI, conduction inhomogeneity; LA, left atrium; PVA, pulmonary vein area; RA, right atrium.

surgery, the application of this tool may help to early identify patients at high risk of PoAF. For instance, if the Electrical Signal Fingerprint Score indicates high CI in SR patients, patients should be long-term-monitored during the post-operative period. Also, preventive strategies may be taken to prevent the development of PoAF. With the ongoing development of high-density electrode arrays for endovascular mapping, less-invasive fingerprints could be constructed in the near future at the electrophysiology laboratory. They can aid in selecting the appropriate ablation approach. For example, when the fingerprint score is too high, the degree of CI is severe and pulmonary vein isolation alone may not be successful in eliminating AF.

Study limitations

Whether Electrical Signal Fingerprint Scores are truly indicative of the AF-related substrate needs to be further investigated. Follow-up of many patients is still ongoing, and therefore, the number of patients is limited for the prediction of especially L-PoAF. However, the preliminary results on PoAF prediction presented in this study show a potential clinical application of the Electrical Signal Fingerprint Score. The number of patients with AF in our study population was too small to compare Electrical Signal Fingerprint Scores among different subtypes of AF. Also, although the study population is not a reflection of the general AF population, 27–33% of the patients who undergo CABG experience AF, indicating that the participants of this study at least represent a group in which AF occurs frequently.[26,27] In addition, this is a single-centre study, and further validation is still needed through subsequent multi-centre studies.

Conclusions

The severity of CI can be accurately quantified by using the Electrical Signal Fingerprint Score, solely employing the electrophysiological characteristics of unipolar EGMs. Electrogram characteristics recorded from the easily accessible RA alone have the best predictive value for the severity of CI of both atria including BB. The next step in developing the Electrical Signal Fingerprint Score as a novel tool is to determine whether this score can be used to identify patients at high risk of onset and/or progression of AF.

Supplementary material

Supplementary material is available at *Europace* online.

Authors' contributions

Z.Y. and M.S.v.S. designed the study, analysed the data, and draft the manuscript. Y.J.H.J.T. contributed to data acquisition and critical

revision of the manuscript. L.P., A.H., P.K., and B.J.J.M.B. contributed to critical revision the manuscript. N.M.S.d.G. contributed to conceptual thinking, study design, data interpretation, manuscript revision, and supervision of the project. All authors contributed to the article and approved the submitted version.

Acknowledgements

The authors thank A.J.J.C. Bogers, MD, PhD; J.A. Bekkers, MD; W.J. van Leeuwen, MD; F.B.S. Oei, MD, PhD; P.C. van de Woestijne, MD; F.R.N. van Schaagen, MD; N.L. Ramdat Misier, BSc; J.H. Amesz, MSc; R.D. Zwijnenburg, MD; M.F.A Bierhuizen, MD; M.C. Roos-Serote, PhD for their contribution to this work.

Funding

N.M.S.d.G. is supported by funding grants from NWO-Vidi (NWO-Vidi is granted via Nederlandse Organisatie voor Wetenschappelijk Onderzoek/Dutch Research Council) (91717339), Biosense Webster USA (ICD 783454), and Medical Delta.

Conflict of interest: None declared.

Data availability

The data that support the findings of this study are available from the corresponding author upon reasonable request.

References

1. Allessie MA, de Groot NMS, Houben RPM, Schotten U, Boersma E, Smeets JL *et al.* Electropathological substrate of long-standing persistent atrial fibrillation in patients with structural heart disease: longitudinal dissociation. *Circ Arrhythm Electrophysiol* 2010;**3**:606–15.
2. Williams SE, Linton NWF, Harrison J, Chubb H, Whitaker J, Gill J *et al.* Intra-atrial conduction delay revealed by multisite incremental atrial pacing is an independent marker of remodeling in human atrial fibrillation. *JACC Clin Electrophysiol* 2017;**3**:1006–17.
3. Pytkowski M, Jankowska A, Maciag A, Kowalik I, Sterlinski M, Szwed H *et al.* Paroxysmal atrial fibrillation is associated with increased intra-atrial conduction delay. *Europace* 2008;**10**:1415–20.
4. de Groot NM, Schalij MJ, Zeppenfeld K, Blom NA, Van der Velde ET, Van der Wall EE. Voltage and activation mapping: how the recording technique affects the outcome of catheter ablation procedures in patients with congenital heart disease. *Circulation* 2003;**108**:2099–106.
5. Miyamoto K, Tsuchiya T, Narita S, Yamaguchi T, Nagamoto Y, Ando S *et al.* Bipolar electrogram amplitudes in the left atrium are related to local conduction velocity in patients with atrial fibrillation. *Europace* 2009;**11**:1597–605.
6. Zhang J, Sacher F, Hoffmayer K, O'Hara T, Strom M, Cuculich P *et al.* Cardiac electrophysiological substrate underlying the ECG phenotype and electrogram abnormalities in Brugada syndrome patients. *Circulation* 2015;**131**:1950–9.
7. Spach MS, Miller W III, Miller-Jones E, Warren RB, Barr RC. Extracellular potentials related to intracellular action potentials during impulse conduction in anisotropic canine cardiac muscle. *Circ Res* 1979;**45**:188–204.
8. Ye Z, van Schie MS, de Groot N. Signal fingerprinting as a novel diagnostic tool to identify conduction inhomogeneity. *Front Physiol* 2021;**12**:375.
9. Lanters EAH, van Marion D, Kik C, Steen H, Bogers AJJC, Allessie MA *et al.* HALT & REVERSE: Hsf1 activators lower cardiomyocyte damage; towards a novel approach to REVERSE atrial fibrillation. *J Transl Med* 2015;**13**:347.
10. van der Does LJME, Yaksh A, Kik C, Knops P, Lanters EAH, Teuwen CP *et al.* QUest for the Arrhythmogenic Substrate of Atrial fibRillation in patients undergoing cardiac surgery (QUASAR study): rationale and design. *J Cardiovasc Transl Res* 2016;**9**:194–201.
11. De Groot NMS, Shah D, Boyle PM, Anter E, Clifford GD, Deisenhofer I *et al.* Critical appraisal of technologies to assess electrical activity during atrial fibrillation: a position paper from the European Heart Rhythm Association and European Society of Cardiology Working Group on eCardiology in collaboration with the Heart Rhythm Society, Asia Pacific Heart Rhythm Society, Latin American Heart Rhythm Society and Computing in Cardiology. *Europace* 2022;**24**:313–30.
12. van Schie MS, Starreveld R, Bogers AJJC, de Groot NMS. Sinus rhythm voltage fingerprinting in patients with mitral valve disease using a high-density epicardial mapping approach. *Europace* 2021;**23**:469–78.
13. van Schie MS, Starreveld R, Roos-Serote MC, Taverne YJHJ, van Schaagen FRN, Bogers AJJC *et al.* Classification of sinus rhythm single potential morphology in patients with mitral valve disease. *Europace* 2020;**22**:1509–19.
14. Roberts-Thomson KC, Kistler PM, Sanders P, Morton JB, Haqqani HM, Stevenson I *et al.* Fractionated atrial electrograms during sinus rhythm: relationship to age, voltage, and conduction velocity. *Heart Rhythm* 2009;**6**:587–91.
15. Teh AW, Kistler PM, Lee G, Medi C, Heck PM, Spence S *et al.* Electroanatomic properties of the pulmonary veins: slowed conduction, low voltage and altered refractoriness in AF patients. *J Cardiovasc Electrophysiol* 2011;**22**:1083–91.
16. Konings KT, Smeets JL, Penn OC, Wellens HJ, Allessie MA. Configuration of unipolar atrial electrograms during electrically induced atrial fibrillation in humans. *Circulation* 1997;**95**:1231–41.
17. Frontera A, Mahajan R, Dallet C, Vlachos K, Kitamura T, Takigawa M *et al.* Characterizing localized reentry with high-resolution mapping: evidence for multiple slow conducting isthmuses within the circuit. *Heart Rhythm* 2019;**16**:679–85.
18. Hocini M, Shah AJ, Nault I, Sanders P, Wright M, Narayan SM *et al.* Localized reentry within the left atrial appendage: arrhythmogenic role in patients undergoing ablation of persistent atrial fibrillation. *Heart Rhythm* 2011;**8**:1853–61.
19. Lanters EA, Yaksh A, Teuwen CP, van der Does LJ, Kik C, Knops P *et al.* Spatial distribution of conduction disorders during sinus rhythm. *Int J Cardiol* 2017;**249**:220–5.
20. Heida A, van der Does WF, van Staveren LN, Taverne YJ, Roos-Serote MC, Bogers AJ *et al.* Conduction heterogeneity: impact of underlying heart disease and atrial fibrillation. *Clin Electrophysiol* 2020;**6**:1844–54.
21. Prabhu S, Voskoboinik A, McLellan AJA, Peck KY, Pathik B, Nalliah CJ *et al.* A comparison of the electrophysiologic and electroanatomic characteristics between the right and left atrium in persistent atrial fibrillation: is the right atrium a window into the left? *J Cardiovasc Electrophysiol* 2017;**28**:1109–16.
22. Heida A, van der Does WFB, van Schie MS, van Staveren LN, Taverne YJHJ, Bogers AJJC *et al.* Does conduction heterogeneity determine the supervulnerable period after atrial fibrillation? *Med Biol Eng Comput* 2023;**61**:897–908.
23. Takagi T, Nakamura K, Asami M, Toyoda Y, Enomoto Y, Moroi M *et al.* Impact of right atrial structural remodeling on recurrence after ablation for atrial fibrillation. *J Arrhythm* 2021;**37**:597–606.
24. van der Does WF, Heida A, van der Does LJ, Bogers AJ, de Groot NM. Conduction disorders during sinus rhythm in relation to atrial fibrillation persistence. *J Clin Med* 2021;**10**:2846.
25. Teuwen CP, Yaksh A, Lanters EA, Kik C, van der Does LJ, Knops P *et al.* Relevance of conduction disorders in Bachmann's bundle during sinus rhythm in humans. *Circ Arrhythm Electrophysiol* 2016;**9**:e003972.
26. Mathew JP, Parks R, Savino JS, Friedman AS, Koch C, Mangano DT *et al.* Atrial fibrillation following coronary artery bypass graft surgery: predictors, outcomes, and resource utilization. *JAMA* 1996;**276**:300–6.
27. Amar D, Shi W, Hogue CW, Zhang H, Passman RS, Thomas B *et al.* Clinical prediction rule for atrial fibrillation after coronary artery bypass grafting. *J Am Coll Cardiol* 2004;**44**:1248–53.